Detection of Breast Tumour Depth using Felt Substrate Textile Antenna

Yusnita Rahayu[1,*], M. Khairon[1], Khairul Najmy Abdul Rani[2], Teguh Praludi[3]

[1] Department of Electrical Engineering Universitas Riau, Pekan Baru, 28293, Indonesia
[2] Advanced Communication Engineering (ACE), Universiti Malaysia Perlis, 01000 Kangar, Perlis, Malaysia
[3] Research Center for Telecommunication BRIN, Indonesia

ARTICLE INFO	ABSTRACT
	Breast cancer is a frightening type of cancer for women globally, including in Indonesia. Early detection of cancer symptoms is crucial to reducing mortality rates. Microwave imaging systems using the ultra-wideband (UWB) can detect objects, particularly in medical diagnosis. The textile antenna is the latest development in antenna technology that can be used on the human body. This antenna can be bent and adjusted to the body's complex shape. This research proposed a textile antenna using the felt dielectric substrate material operating at 3.8 GHz. The simulation results showed a return loss value of -47.5138 dB and a bandwidth of 1.4 GHz. The antenna was also tested on a breast phantom with a tumour scenario, showing higher amplitude in the quadrant with the tumour. The fabrication was done manually through laser cutting and heat-assisted bonding. The antenna made of the felt substrate material could detect breast tumours' multiple depths or layers using the graphical user interface (GUI) programming.

1. Introduction

Breast cancer is the most common cancer in women worldwide [1]. According to data from the Ministry of Health of the Republic of Indonesia, there were a total of 68,858 new cases of breast cancer in Indonesia in 2020, indicating approximately 16.6% of the total new cancer cases of 396,914 cases across all regions in Indonesia [2]. Therefore, early detection of breast cancer is the key to improving the chances of recovery [3,4]. Currently, mammography is the most common method used for the early detection of breast cancer [5]. However, mammography has limitations, such as variability in radiographic interpretation and low risk of ionizing radiation exposure [6,7]. Therefore, the best chance to detect a tumour with a mammogram is when the tumour has reached the late stage of classification [8].

As an alternative, textile antennas made of felt material can be used as a non-invasive and non-radiation solution for detecting the depth of breast tumours. Textile antennas are flexible antennas made of textile material and can be configured in various shapes and sizes [9-11]. This study chose a

---

textile antenna made of felt material because it has several advantages, such as good mechanical strength and the ability to capture microwaves effectively. In addition to using the felt textile antenna, breast tumour depth detection technology is also developed by utilizing UWB frequency [11-14]. UWB technology transmits signals with an extremely wide frequency spectrum [15]. In breast tumour detection applications, UWB frequency has an advantage in obtaining detailed images of breast tissue, including detecting tumours at greater depths [15-17]. The first regulation for UWB technology was issued by the Federal Communications Commission (FCC) in 2002. The FCC defined UWB as a technology with a bandwidth ≥ 500 MHz and an operating frequency range of 3.1-10.6 GHz. As a new and innovative technology, UWB has tremendous potential to become a solution in various fields, such as communication, medical imaging, and explosive detection [18].

Due to the limited number of research works on textile antenna for breast tumour depth detection, especially in 2D/3D visualization, motivates the authors to contribute to this. This work's significance is that the textile antenna can detect and visualize the breast tumour depth in 2D/3D images. The method of detecting the depth of breast tumours using a felt textile antenna is based on the dielectric properties of the tumour tissue and its surroundings when electromagnetic waves pass through breast tissue. The data obtained is then extracted from the waves the antenna receives using signal processing techniques. Our main objective is to see how a GUI program displays the detection results in a 3D visualization. Measurements were taken on a phantom breast model with and without tumours at different depths using two textile antenna elements operating at UWB frequencies. The antenna design was created using CST Microwave Studio software, while the fabrication measurements of the felt textile antenna were taken using a Vector Network Analyzer (VNA). The measurement results were used to evaluate the antenna's performance in detecting the depth of tumours in breast tissue and serve as the basis for developing better and more effective early breast cancer detection technologies.

2. Methodology
2.1 Antenna Specifications

The antenna design begins with identifying the critical specifications used as parameters for simulation results. The specifications for the simulated antenna results in this study are shown in Table 1.

Table 1 contains the parameter specifications that will be used in designing a textile antenna. These parameters include the operating frequency of 3.1 - 10.6 GHz, which is the working frequency of ultra-wideband technology. In addition, the impedance value must be 50 Ω, and the return loss must be less than or equal to -10 dB for the antenna to work properly [18].

Table 1
Specifications of textile antenna

Frequency	Impedance	Return loss	Bandwidth
(3.1-10.6 GHz)	50 Ω (SMA Connector Coaxial)	≤ -10 dB	Minimum ≥ 500 MHz

2.2 Antenna Design

The substrate used in this study is felt substrate material with specifications shown in Table 2.

Table 2
Substrate specifications

Type of Substrate	Felt
Relative Dielectric Constant (ε_r)	1.44
Dielectric Loss Tangent (tan δ)	0.044
Substrate Thickness (h)	1 mm

The proposed dimensions of the antenna element are calculated as follows. The width (*W*) and length (*L*) of the substrate are calculated using Eq. (1) to Eq. (4) below [19] :

$$W = \frac{c}{2f_0\sqrt{\frac{\varepsilon_r+1}{2}}} \tag{1}$$

$$\Delta L = \frac{c}{2f_0\sqrt{\varepsilon_r}} - 0.824h\left(\frac{(\varepsilon_{eff}+0.3)\left(\frac{w}{h}+0.264\right)}{(\varepsilon_{eff}-0.258)\left(\frac{w}{h}+0.8\right)}\right) \tag{2}$$

$$L_{eff} = \frac{3 \times 10^8}{2 \times 3.1 \times 10^8\sqrt{1.274}} \tag{3}$$

$$L = L_{eff} - 2\,\Delta L \tag{4}$$

Where,
W : Width of Conductor (mm)
ε_r : Dielectric Constant
c : Light Velocity (3×10^8 m/s)
f_0 : Frequency (Hz)

The dimensions of the antenna ground can be calculated using the following Eq. (5) and Eq. (6) below [20]:

$$Wg = 6h + W\,patch \tag{5}$$

$$Lg = 6h + W\,patch \tag{6}$$

Where,
h : Substrate Thickness
Wg : Antenna Ground Width
Lg : Antenna Ground Length
The width of the antenna feeding channel can be calculated using Eq. (7) below:

$$W_f = 2 \times h\pi \times [B - 1 - \ln(2B - 1) \times \varepsilon_r - 12\varepsilon_r \times [\ln(B - 1) + 0.39 - 0.61\varepsilon_r \tag{7}$$

2.3 Antenna Architecture

The characterization results of the antenna showed a frequency of 3.8 GHz, a return loss of -7.513 dB, and it operates within a bandwidth of 1.5 GHz at a frequency range of 2.983 − 4.336 GHz. Figure 1 shows the textile antenna design using CST software.
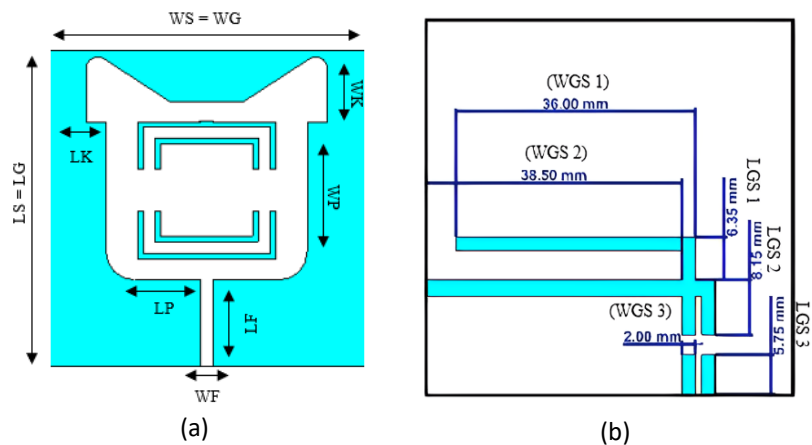
(a)   (b)

Fig. 1. The final design of the textile antenna

3. Results and Discussion

3.1 Antenna Fabrication

In this research, a textile antenna operating at 3.8 GHz with a bandwidth > 500 MHz was developed, as shown in Figure 2. The feeding technique used was a microstrip feed line.

(a)   (b)

Fig. 2. Fabricated textile antenna (a) Front view and (b) Back view

Based on the characterization process carried out during the design, the final proposed antenna dimensions were obtained, as shown in Table 3.

Table 3
Dimensions of the proposed textile antenna

Parameter	Dimension (mm)
WP (Width of the patch)	38.5
LP (Length of patch)	30
WG Groundplane = WS Substrate	55
LG Groundplane = LS Substrate	55
WF Stripline	2
LF Stripline	16
WK Antenna Ear	3.50
LK Antenna Ear	9.31
WGS 1 (Width of ground slot 1)	36
WGS 2 (Width of ground slot 2)	38.50
WGS 3 (Width of ground slot 3)	2
LGS 1 (Length of ground slot 1)	6.35
LGS 2 (Length of ground slot 2)	8.15
LGS 3 (Length of ground slot 3)	5.75

Figure 2 is the fabricated antenna in both front and back views. After fabrication, the antenna was measured using a pocket VNA measurement instrument to assess the variation between the simulation results obtained from the CST software and the fabricated antenna results on the specific parameters. The comparison of the proposed antenna simulation and fabrication outcomes is illustrated in Figure 3.
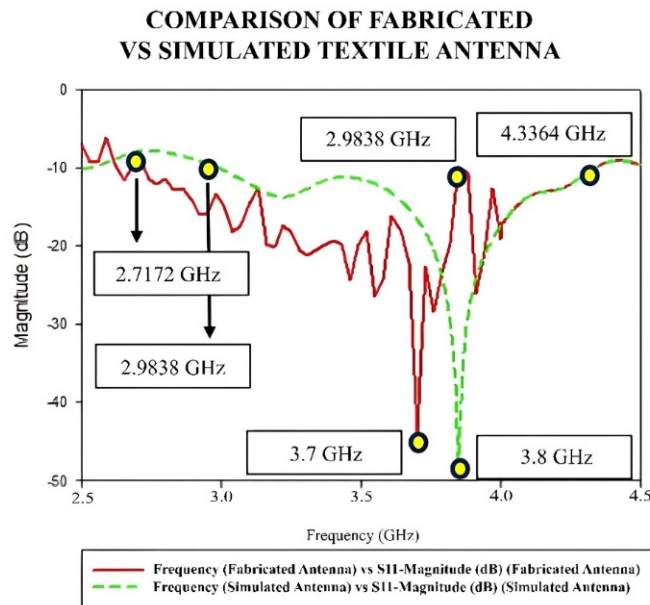

Fig. 3. Comparison of return loss for both fabricated and simulated antenna

Figure 3 shows the simulated return loss of -47.513 dB at a frequency of 3.8 GHz. Meanwhile, the measured return loss was -43.6714 dB at a frequency of 3.7 GHz. The measurement results indicated a frequency shift of 100 MHz compared to the simulation results. Then, the simulated antenna bandwidth was 1.4 GHz at a frequency range of 2.9838 GHz to 4.3364 GHz, while the fabricated antenna bandwidth was 1.14 GHz at a frequency range of 2.7172 GHz to 3.8612 GHz. Using Eq. (8), the error value between the simulation and fabricated antenna measurement results could be determined as follows.

$$Error \ (f) = \left| \frac{f_c \ Measurement - f_c \ Simulation}{f_c \ Simulation} \right| \times 100\% \tag{8}$$

$$Error \ (f) = \left| \frac{3.7 - 3.8}{3.8} \right| \times 100\% = 0.026 \ \% \tag{9}$$

The error value obtained through Eq. (8) was 0.026%. This error value is minimal, so it can be stated that the fabricated antenna was suitable for detection purposes.

3.2 Antenna Flexibility Testing

Flexibility testing was carried out to see the antenna's performance in various forms of deformation based on the shape of the applied detection object. Flexibility testing was done by bending at four angles: 30, 40, 50, and 60 degrees. The test was carried out by attaching the antenna to the cylinder tube and following the shape of the cylinder tube. Figure 4a-4d shows the method used for the measurement, whereas Figure 5a-5d shows the comparison of return loss between the fabricated antenna and the simulated antenna due to the bending effect.
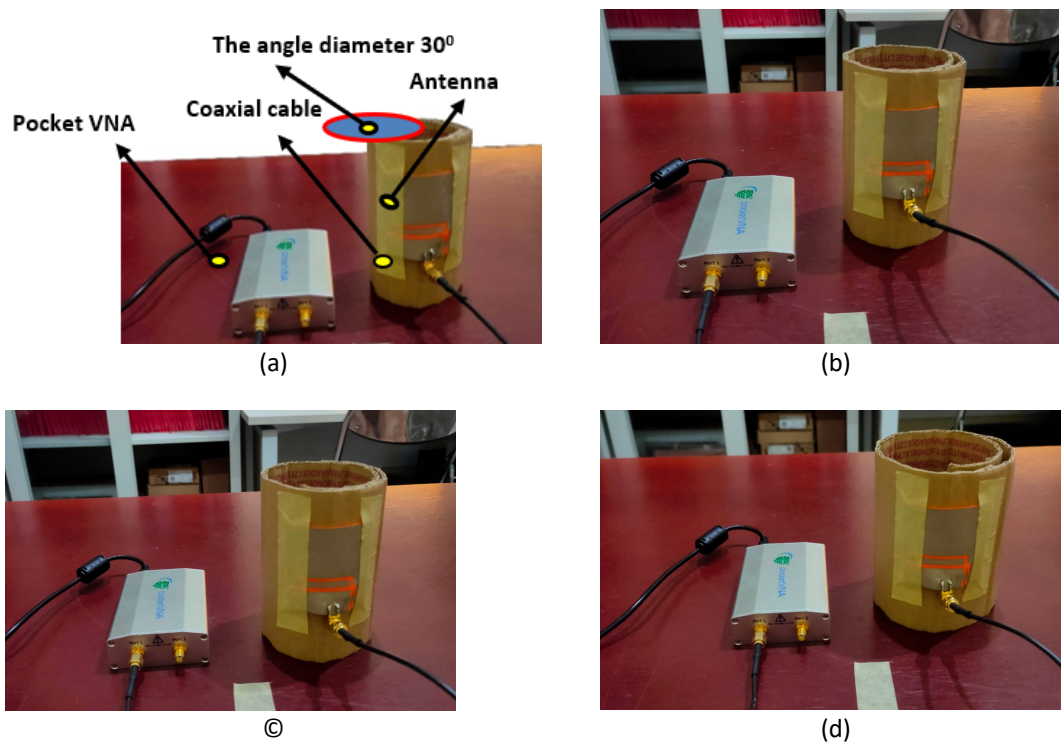

Fig. 4. Antenna bending test method (a) 0° (b) 40° (c) 50° (d) 60°
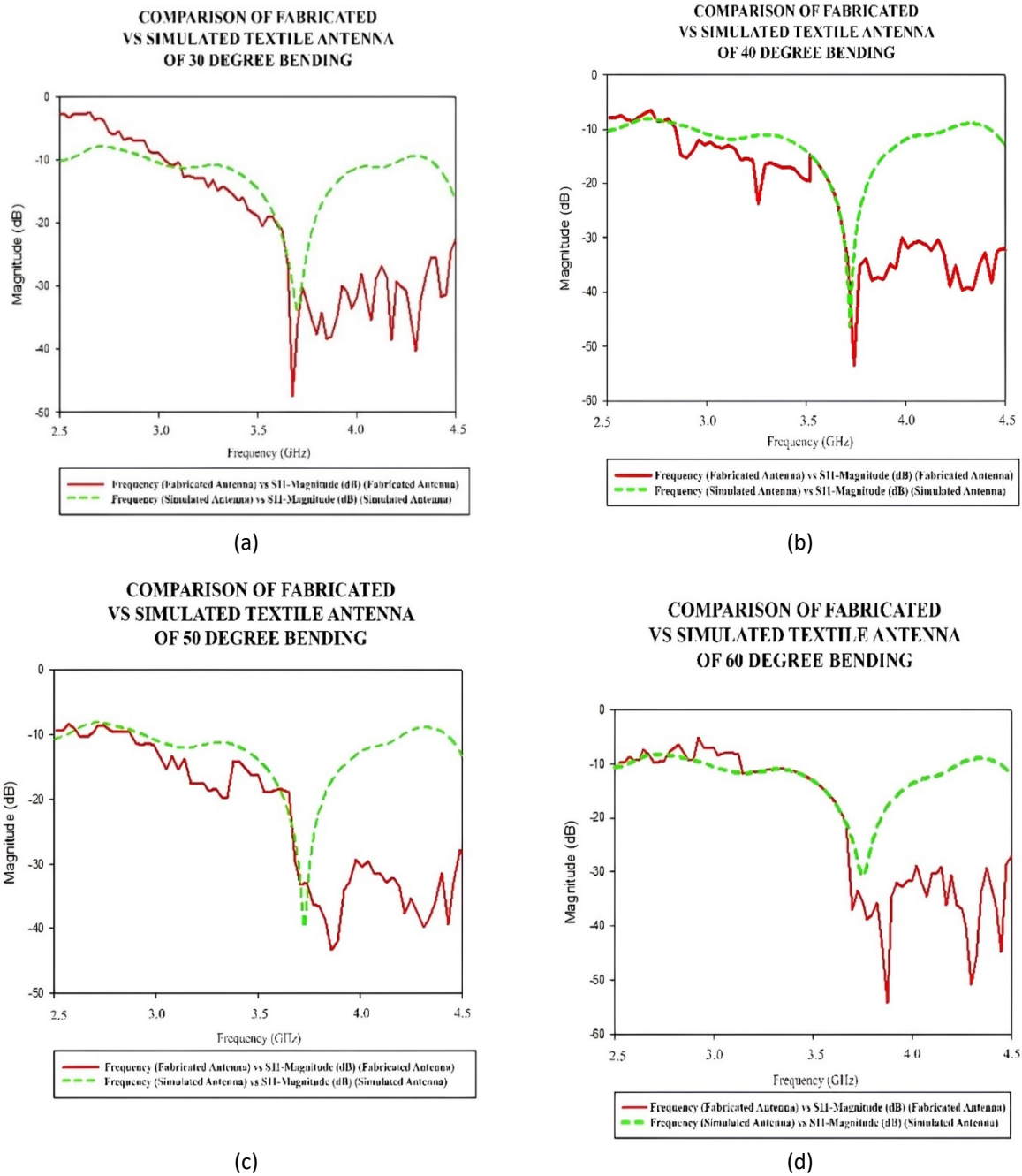
Fig. 5. Bending effect to return loss (a) 30° (b) 40° (c) 50° (d) 60°

Table 4 shows the fabricated and simulated antennas' frequency and return loss values. The measured return loss is getting lower for each bending position. However, the frequency centre is only shifted around 100 MHz. The obtained values do not indicate significant differences, indicating that the antenna can operate at frequencies that are not significantly different when subjected to bending tests for flexibility evaluation of textile antennas in this study.

Table 4
Comparison of the return loss of textile antenna on bending structure

Bending Angle (Degree)	Frequency (GHz)		Return loss (dB)	
	Simulated	Fabricated	Simulated	Fabricated
30	3.7	3.6	-33.7997	-47.4714
40	3.7	3.7	-46.4670	-53.7429
50	3.7	3.8	-39.7640	-43.4571
60	3.75	3.8	-30.7940	-54.0514

3.3 Tumour Detection in Breast Phantoms
3.3.1 Simulation of tumour detection in breast phantom

Breast phantom simulation aims to compare signal amplitude results based on the location and reference of detection with a textile antenna for breast modelling. Antenna simulation with breast phantom was done with two conditions: breast phantom with tumour and without tumour, as illustrated in Figure 6. The tumour is modelled as a small circle in quadrant one, as shown in Figure 6(a). Four antennas are placed around the breast phantom. The breast phantom is divided into four quadrants. The 1st quadrant is the tumour position, the 2nd quadrant is the opposite side, the 3rd and 4th quadrants are up and down.
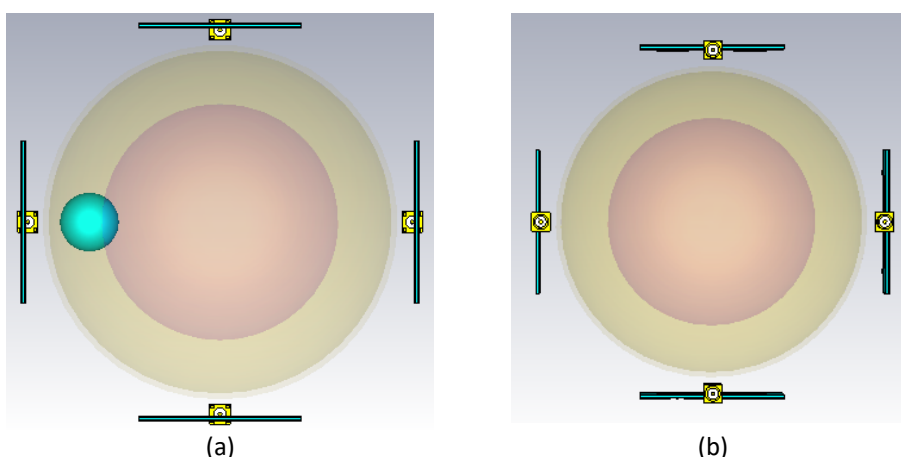

(a)   (b)

Fig. 6. Antenna position on breast phantom (a) With tumour and (b) Without tumour

Figure 7 shows a time domain amplitude comparison between breast phantom with and without tumour. The results showed that the presence of a tumour in the breast phantom (Figure 7(a)) caused an increase in the waveform amplitude in the time domain compared to the breast phantom without a tumour. This study implies that an increase in the waveform amplitude in the time domain can indicate the presence of a breast tumour in medical diagnosis.
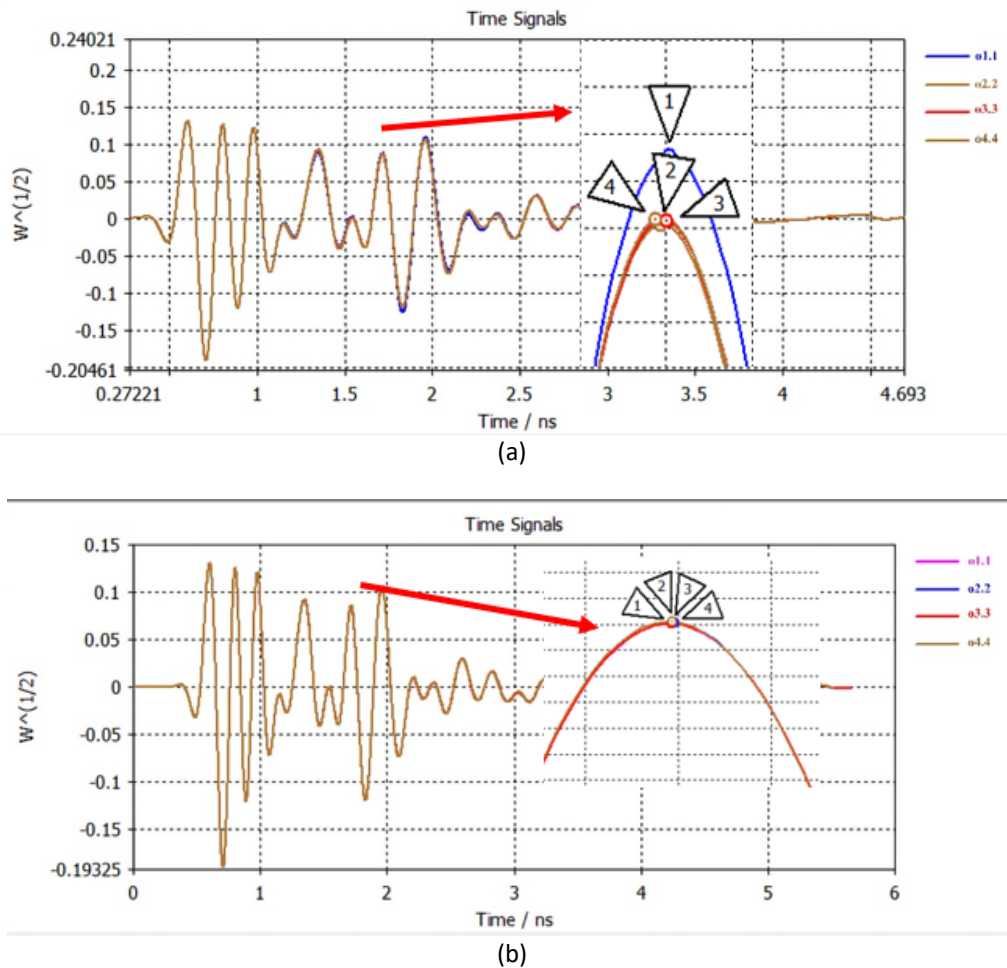
Fig. 7. Time domain amplitude of breast phantom (a) With tumour (b) Without tumour

Table 5 shows that the amplitude value in quadrant 1 was higher than the amplitude value in the other quadrants at 1.9609 ns. Quadrant 2 had the lowest amplitude due to its position opposite quadrant 1, with a tumour. In contrast, the amplitude value in each quadrant without a tumour was reduced due to the absence of obstructions that affected the reflection coefficient.

Table 5
Amplitude value of time domain simulated breast phantom with and without tumour

Quadrant	Time (ns)		Amplitude (V)		Comparator Amplitude (Quadrant 1) (V)
	Tumour	Without Tumour	Tumour	Without Tumour	Tumour
1	1.9609	1.9593	10.907×10^{-5}	10.602×10^{-5}	10.907×10^{-5}
2	1.959	1.9596	10.613×10^{-5}	10.608×10^{-5}	10.907×10^{-5}
3	1.9603	1.9592	10.628×10^{-5}	10.602×10^{-5}	10.907×10^{-5}
4	1.9576	1.9594	10.637×10^{-5}	10.608×10^{-5}	10.907×10^{-5}

3.3.2 Fabrication of tumour detection in breast phantom

A phantom is an artificial replica of an organ or body part designed to mimic the physical structure and properties of the original body part [21]. The breast phantom was maintained in shape for six weeks. The breast phantom was then inserted with a breast tumour of 1 mm at three depth conditions of 20, 40, and 60 mm. The breast phantom will be divided into four quadrants, each tested

at different depths. Figure 8(a) shows the shape of the fabricated breast phantom, whereas Figure 8(b) shows the fabricated tumour.
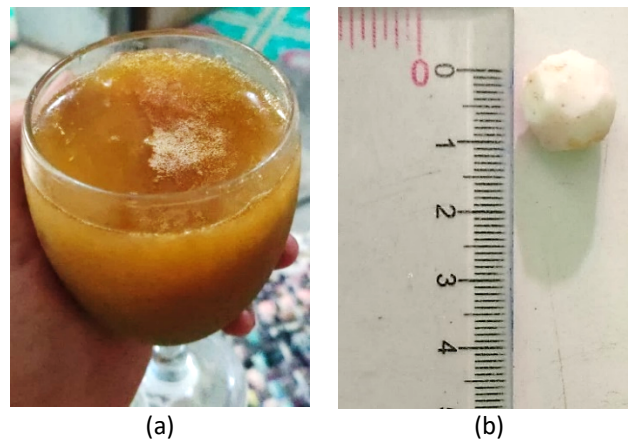

(a)   (b)

Fig. 8. Phantom fabrication results (a) Breast and (b) Tumour

The tumour detection process was done using a Pocket Vector Network Analyzer (VNA) tool. The tool measured the value of the transmission coefficient on the antenna., In this case, measurements were made to take real and imaginary S_{21} data (Frequency Domain). The S_{21} data was processed through Phyton and MATLAB programming to obtain the depth of the breast tumour. A transmitter antenna was placed in the centre of the breast model, whereas a receiver antenna was placed in each quadrant to detect the breast tumour. Figure 9 shows the measurement setup of the textile antenna with the breast phantom.
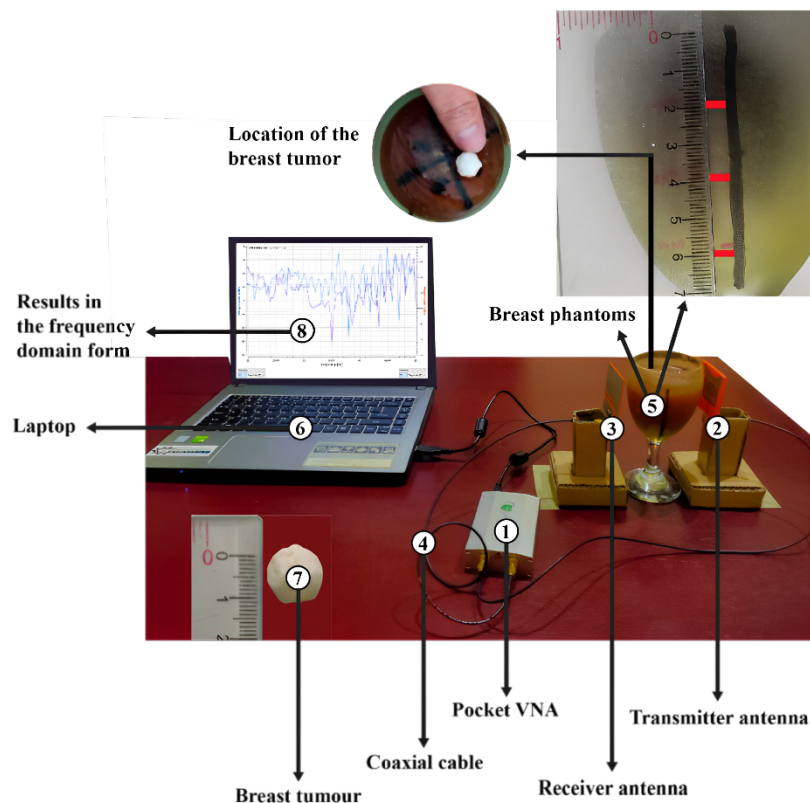

Fig. 9. Antenna measurement setup using pocket VNA

Figure 10 shows the time domain amplitude comparison of textile antenna measurements of breast phantoms with tumours at a predetermined depth and breast phantoms without tumours. In this case, quadrant 1 is the area with the tumour at various depths of 20 mm, 40 mm, and 60 mm. From the figure, the amplitude of the phantom without tumours at 1.798 ns was 0.0025 V.
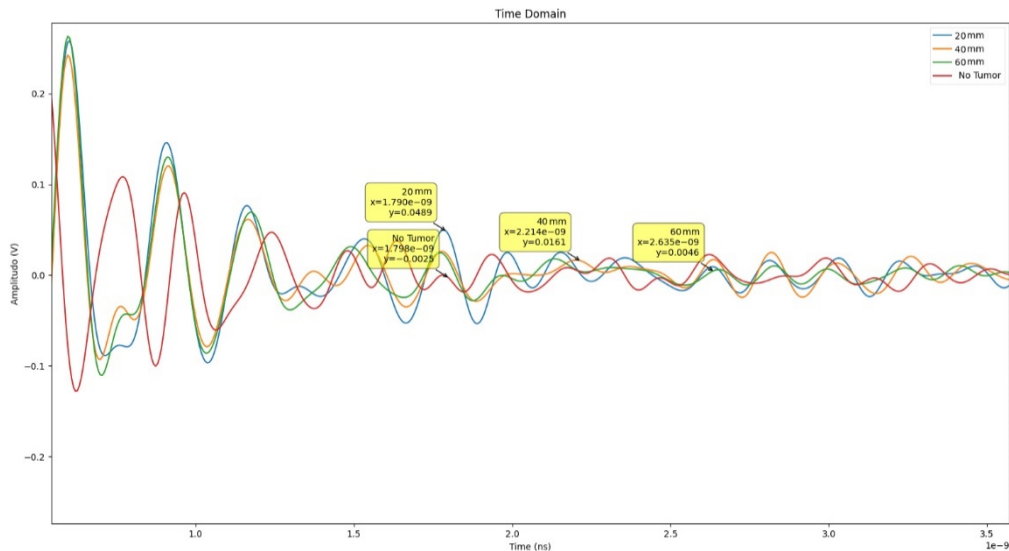

Fig. 10. The amplitude comparison of the time domain between the condition without and with a tumour at depths of 20 mm, 40 mm, and 60 mm

Moreover, the amplitudes at a depth of 20 mm, 40 mm, and 60 mm spiked. The amplitude of the graph at a depth of 20 mm at a time of 1.790 ns was 0.0489 V, at a depth of 40 mm at a time of 2.214 ns was 0.0161 V, and at a depth of 60 mm at a time of 2.635 ns was 0.0046 V. Comparison of amplitude values in breast phantoms with tumours at different depths and without tumour are listed in Table 6.

Table 6
Amplitude comparison in the time domain

Tumour Depth	Time (ns)	Amplitude (V)	Comparator Amplitude (Without Tumour)	Amplitude Difference (V)
20 mm	1.790	0.0489	0.0025	0.0464
40 mm	2.214	0.0161	0.0025	0.0136
60 mm	2.635	0.0046	0.0025	0.0021
Without Tumour	1.798	0.0025	0.0025	-

Table 6 compares the amplitude at tumour depth in breast phantoms with and without tumour. The analysis shows that the amplitude spiked at a depth of 20 mm was larger than that at the depths of 40 mm and 60 mm, with amplitude differences of 0.0464 V. At the depth of 20 mm, the larger amplitude difference was due to the larger wave amplitude as there was no tissue resistance and the wave reflected from the tumour was also larger at a shallower depth. The time domain signal analysis shows the amplitude difference between the conditions with and without tumours and can be used to detect and locate tumours in the breast.

3.3.3 Comparative analysis of amplitude in time domain

Amplitude comparison between the simulated and fabricated antenna on the breast phantom can be seen in Table 7 below.

Table 7
Amplitude comparison of simulated and fabricated antenna on a breast phantom

Condition	Simulation		Fabrication	
	Time (ns)	Amplitude (V)	Time (ns)	Amplitude (V)
Tumour	1.9603	0.10628	1.790	0.0489
Without Tumour	1.9592	0.10602	1.798	0.0025

The main cause of the amplitude difference between the simulation and fabrication results on the breast phantom was that the fabrication process was complicated and required precise tools. In addition, the fabrication process was limited to the dosage and materials used, which made the fabrication results worse. The different epsilon in the breast phantom is also contributed. Therefore, epsilon testing was necessary to improve the validity and quality of the breast phantom. Nonetheless, the proposed antenna could still detect the depth and tumour in the breast phantom.

3.4 Breast Tumour Depth Detection in GUI Form

Figure 11 shows how the Graphical User Interface (GUI) provided by the MATLAB program processes data to determine the depth of a tumour in a breast phantom and visualizes it in 2D and 3D forms. The breast phantom is a breast model used to test the program's ability to detect tumours. The GUI will receive raw data about the breast condition and then perform data processing using machine learning to determine the depth of the tumour inserted into the breast phantom.
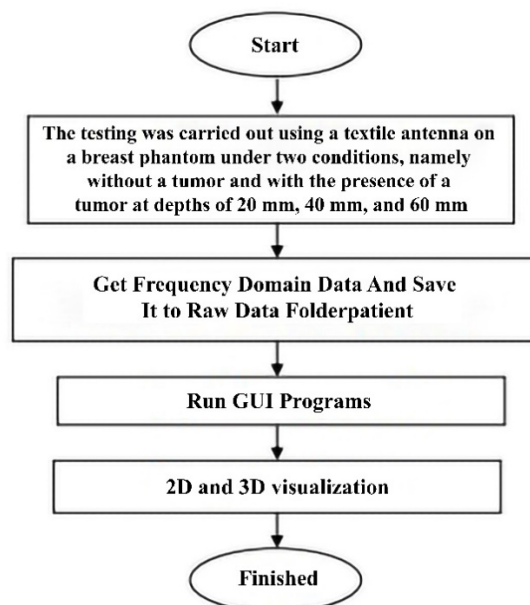

Fig. 11. Flowchart for using the GUI Program

The application of the GUI in this study was carried out by obtaining raw data on the results of tumour detection by the antenna on the breast. The results of data execution were then presented

as shown in Table 8, which consists of True (1) and False (0) values. Visualization of the tumour presence point can be seen in 2D form or 3D form. In this study, tumour data was located in Quadrants 1, 2, and 3, as shown in Table 8. This table shows that the program could provide accurate information about the location and depth of the tumour in the fabricated breast phantom.

Table 8
Tumour output data

Output	Quadrant 1			Quadrant 2			Quadrant 3			Quadrant 4		
	20 mm	40 mm	60 mm	20 mm	40 mm	60 mm	20 mm	40 mm	60 mm	20 mm	40 mm	60 mm
Without Tumour	0	1	1	1	1	0	1	0	1	1	1	1
Depth of Breast Tumour	1	0	0	0	0	1	0	1	0	0	0	0

Figure 12 shows the results obtained by inserting several tumours in each quadrant at different depths of 20 mm, 40 mm, and 60 mm, respectively. The graphical visualization was made to show the shape of the breast and the coloured dots of the detected tumours. Green dots were tumours in the Quadrant 1 at the depth of 20 mm.
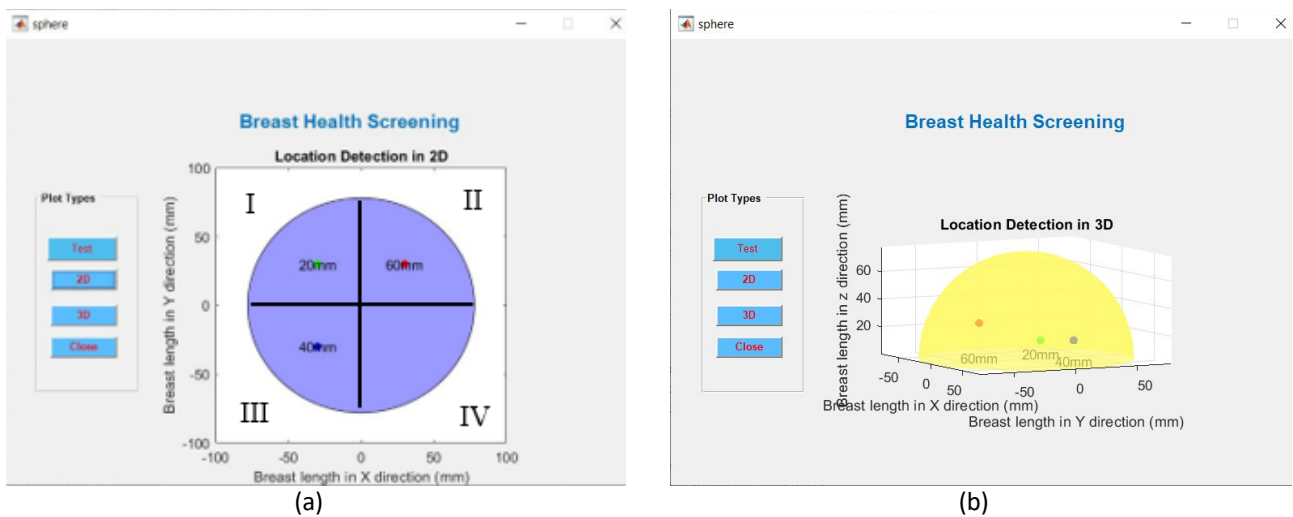

(a)	(b)

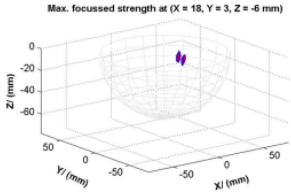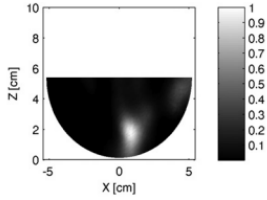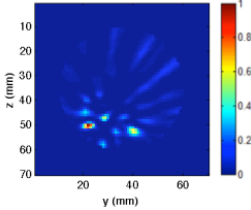**Fig. 12.** Location of 3 tumours on the GUI (a) 2D view and (b) 3D view

Table 9 compares breast tumour detection analysis studies, including information about the types of antennas used and the final results of the studies, which can differ between 2D and 3D visualizations. In this work, detecting the depth of breast tumours using machine learning techniques was applied and had advantages over methods in previous studies. The previous studies used other medical image reconstructions such as FBP, DAS & MAMI, DMAS, MSE & SSIM, and TR (Transformed Radon). The advantages of this work are as follows:
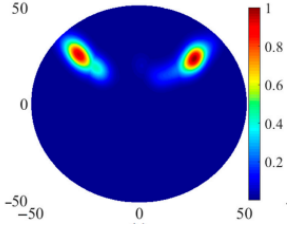
i. The ability to generate more accurate models in detecting breast tumours, as it can learn complex patterns from medical data and account for interactions between different features in medical images [21].

ii. The ability to perform faster medical image reconstruction by utilizing GPU and TPU technology in the training and inference process of the model [22].

iii. The ability to generate more stable models that can be improved as more data becomes available, as machine learning models can be easily updated when new data becomes available. [23]

Table 9
Comparison of simulated amplitude and fabricated breast phantom results

Author	Depth Detection Technique	3D and 2D Visualization
Maciej Klemm, Ian J. Craddock, Jack A. Leendertz, Alan Preece, and Ralph Benjamin	This study describes the process of breast tumour detection using the radar method with DAS (Delay-and-Sum) and MAMI (Modified Almost Matched-Filter Image) algorithms. Artificial breast tissue samples were prepared and then scanned using a hemispherical antenna array-based radar system to generate radar images. The radar image data was processed using DAS and MAMI algorithms, and the performance of both algorithms was compared with statistical analysis and visualization. Furthermore, the detected tumour data was analysed to determine the depth of the tumour in the breast tissue, and visualization of the tumour detection and depth results was created.	
Malyhe Jalilvand, Xuyang Li, Lukasz Zwirello, Thomas Zwick	This research used a 16-element antenna array with a multistatic scenario for breast depth measurement. The measurement results were processed using the FBP (Filtered Back-Projection) image processing technique to produce a breast surface image with depth. The reconstruction process was performed by processing the 2D image into a 3D image using the FBP algorithm.	
E Porter, H. Bahrami, A. Santorelli *et al.,*	The first step in this study is the collection of breast scan data from volunteers over 28 days using a portable tabletop prototype. Then, each data is processed using the DMAS (Delay-Multiply and Sum) algorithm to generate a microwave imaging micro image that shows the electromagnetic distribution within the breast tissue. Next, the original and reconstructed images are compared using the MSE (Mean Squared Error) and SSIM (Structural Similarity Index) methods to evaluate the reconstruction quality.	

Sarmad Nozad Mahmood, Asnor Juraiza Ishak, Tale Saeidi, Azura Che Soh, Ali Jalal, Muhammad Ali Imran, and Qammer H. Abbasi	This journal presents a study on textile antennas that can be used for breast tumour detection and wireless signal transmission. The antenna design must consider the effects on the human body tissue, which has high power loss and permittivity. Various wearable antenna shapes, such as PIFA, dipole, and CPIF, can be used. During the testing phase, the antenna is tested with and without breast tumours, and its performance is evaluated in both on-body and off-body conditions. Two stages are performed to detect the tumour's depth: the Single Channel Time Reversal (SCD) and the Robust Time Reversal (TR) algorithm. SCD obtains the required acquisition data, while TR is used for tumour image reconstruction. The TR algorithm is implemented using MATLAB software. The results of the study show that this textile antenna has the potential to detect breast tumours accurately and can be integrated into a wireless body network.	
Yusnita Rahayu, M Khairon, Khairul Najmy Abdul Rani and Teguh Praludi	The tumour detection process is performed using a Pocket Vector Network Analyzer (VNA) device, which measures the transmission coefficient values on the antenna. This measurement collects real and imaginary S21 data in the frequency domain. The IFFT algorithm transforms the frequency domain data into the time domain. The time domain data is labelled and used as a datasheet for processing through the PNN algorithm with 1000 data using machine learning techniques. The output data from the machine learning process is visualized in 2D and 3D with the help of GUI programming.	

4. Conclusions

This research proposed a textile UWB antenna with a bandwidth of >500 MHz at a frequency of 3.8 GHz. The proposed antenna used a microstrip feeding technique with felt as the substrate, which has a dielectric constant 1.44. Simulation results show that the textile antenna had a return loss value of -47.513 dB and a bandwidth value of 1.4 GHz in the frequency range of 2.98 - 4.33 GHz. Simulation results also show that the antenna can detect tumours at a certain depth by increasing the amplitude value in the quadrant where the tumour was located. The fabricated breast phantom had the best return loss at a frequency of 3.7 GHz, which was -43.6714 dB, and the comparison error value between the simulation and fabrication measurements was 0.026%. In addition, the fabrication antenna had good flexibility by having a wider antenna bandwidth ratio during the bending process compared to the simulation results. The tumour detection was measured using the Pocket Vector Network Analyzer (VNA) based on the real and imaginary S21 data. The S21 data was then processed using a programming series to display the breast tumour's depth in 2D/3D images. In sum, the felt substrate textile antenna could be used as an alternative tool for breast tumour detection.

References

[1] Rahayu, Yusnita, M. F. Hilmi, and T. Odih. "Wearable antenna for time-domain breast tumor detection." *International Journal of Technology* 12, no. 6 (2021). https://doi.org/10.14716/ijtech.v12i6.5187

[2] Nirwana, Betanuari Sabda, Khofidhotur Rofiah, Alfika Awatiszahro, Sri Mulyani, and Hesti Rahayu. "The Effect of Counseling About SADARI with Demonstration Methods on WUS Skills (Women of Childbearing Age)." *Journal for Quality in Public Health* 6, no. 1 (2022): 292-295.

[3] Çalışkan, Rabia, S. Sinan Gültekin, Dilek Uzer, and Özgür Dündar. "A microstrip patch antenna design for breast cancer detection." *Procedia-Social and Behavioral Sciences* 195 (2015): 2905-2911. https://doi.org/10.1016/j.sbspro.2015.06.418

[4] Kahwaji, Ali, Haslina Arshad, Shahnorbanun Sahran, Ali Garba Garba, and Rizuana Iqbal Hussain. "Hexagonal microstrip antenna simulation for breast cancer detection." In *2016 international conference on industrial informatics and computer systems (CIICS)*, pp. 1-4. IEEE, 2016. https://doi.org/10.1109/ICCSII.2016.7462400

[5] Rahayu, Yusnita, M. F. Hilmi, and Huriatul Masdar. "A novel design rectangular UWB antenna array for microwave breast tumor detection." In *2019 16th International Conference on Quality in Research (QIR): International Symposium on Electrical and Computer Engineering*, pp. 1-5. IEEE, 2019. https://doi.org/10.1109/QIR.2019.8898292

[6] Jalilvand, Malyhe, Xuyang Li, Lukasz Zwirello, and Thomas Zwick. "Ultra wideband compact near-field imaging system for breast cancer detection." *IET Microwaves, Antennas & Propagation* 9, no. 10 (2015): 1009-1014. https://doi.org/10.1049/iet-map.2014.0735

[7] Vijayasarveswari, V., M. Jusoh, T. Sabapathy, Rafikha Aliana, S. Khatun, Z. A. Ahmad, and Mohamed Nasrun Osman. "Performance verification on UWB antennas for breast cancer detection." In *MATEC Web of Conferences*, vol. 140, p. 01004. EDP Sciences, 2017. https://doi.org/10.1051/matecconf/201714001004

[8] Tayel, Mazhar B., and Hazem A. Elfaham. "Microwave SAR as a tool for tumor determination." In *2016 11th International Conference on Computer Engineering & Systems (ICCES)*, pp. 207-211. IEEE, 2016. https://doi.org/10.1109/ICCES.2016.7822001

[9] Aydın, Emine Avşar. "A Novel Flexible Microstrip Patch Antenna with Different Conductive Materials For Telemedicine and Mobile Biomedical Imaging Systems." (2021). https://doi.org/10.21203/rs.3.rs-664932/v1

[10] Mahmood, Sarmad Nozad, Asnor Juraiza Ishak, Ali Jalal, Tale Saeidi, Suhaidi Shafie, Azura Che Soh, Muhammad Ali Imran, and Qammer H. Abbasi. "A Bra Monitoring System Using a Miniaturized Wearable Ultra-Wideband MIMO Antenna for Breast Cancer Imaging." *Electronics* 10, no. 21 (2021): 2563. https://doi.org/10.3390/electronics10212563

[11] Mahmood, Sarmad Nozad, Asnor Juraiza Ishak, Tale Saeidi, Azura Che Soh, Ali Jalal, Muhammad Ali Imran, and Qammer H. Abbasi. "Full ground ultra-wideband wearable textile antenna for breast cancer and wireless body area network applications." *Micromachines* 12, no. 3 (2021): 322. https://doi.org/10.3390/mi12030322

[12] Huda, Yusron Tri, Tommi Hariyadi, and Budi Mulyanti. "Rancang Bangun Antena Unidirectional Ultra-Wideband dengan Desain Fork-Shaped Tuning Stub menggunakan Bahan Dielektrik Fr-4." *ELECTRANS* 14, no. 1: 60-67.

[13] Banu, MA Shahira, S. Vanaja, and S. Poonguzhali. "UWB microwave detection of breast cancer using SAR." In *2013 International Conference on Energy Efficient Technologies for Sustainability*, pp. 113-118. IEEE, 2013.

[14] Hossain, Kabir, Thennarasan Sabapathy, Muzammil Jusoh, Shen-Han Lee, Khairul Shakir Ab Rahman, and Muhammad Ramlee Kamarudin. "Negative index metamaterial-based frequency-reconfigurable textile CPW antenna for microwave imaging of breast cancer." *Sensors* 22, no. 4 (2022): 1626. https://doi.org/10.3390/s22041626

[15] Rahayu, Yusnita, Tharek Abd Rahman, Razali Ngah, and Peter S. Hall. "Ultra wideband technology and its applications." In *2008 5th IFIP International Conference on Wireless and Optical Communications Networks (WOCN'08)*, pp. 1-5. IEEE, 2008. https://doi.org/10.1109/WOCN.2008.4542537

[16] Acti, Tess, Alford Chauraya, Shiyu Zhang, William G. Whittow, Rob Seager, J. C. Vardaxoglou, and Tilak Dias. "Embroidered wire dipole antennas using novel copper yarns." *IEEE Antennas and Wireless Propagation Letters* 14 (2014): 638-641. https://doi.org/10.1109/LAWP.2014.2371338

[17] Chen, Zhijian, Weisi Zhou, and Jingsong Hong. "A miniaturized MIMO antenna with triple band-notched characteristics for UWB applications." *IEEE access* 9 (2021): 63646-63655. https://doi.org/10.1109/ACCESS.2021.3074511

[18] Mahmood, Sarmad Nozad, Asnor Juraiza Ishak, Alyani Ismail, Azura Che Soh, Zahriladha Zakaria, and Sameer Alani. "ON-OFF body ultra-wideband (UWB) antenna for wireless body area networks (WBAN): a review." *IEEE Access* 8 (2020): 150844-150863. https://doi.org/10.1109/ACCESS.2020.3015423

[19] Sakib, Nazmus, Siti Noorjannah Ibrahim, Muhammad Ibn Ibrahimy, Md Shazzadul Islam, and MM Hasan Mahfuz. "Design of microstrip patch antenna on rubber substrate with DGS for WBAN applications." In *2020 IEEE Region 10 Symposium (TENSYMP)*, pp. 1050-1053. IEEE, 2020. https://doi.org/10.1109/TENSYMP50017.2020.9230707

[20] Yeo, Junho, and Jong-Ig Lee. "Design of a high-sensitivity microstrip patch sensor antenna loaded with a defected ground structure based on a complementary split ring resonator." *Sensors* 20, no. 24 (2020): 7064. https://doi.org/10.3390/s20247064

[21] Yang, Lei, Junfeng Fan, Yanhong Liu, En Li, Jinzhu Peng, and Zize Liang. "A review on state-of-the-art power line inspection techniques." *IEEE Transactions on Instrumentation and Measurement* 69, no. 12 (2020): 9350-9365. https://doi.org/10.1109/TIM.2020.3031194

[22] Islam, Mohammad Tariqul, Md Tarikul Islam, Md Samsuzzaman, Salehin Kibria, and Muhammad EH Chowdhury. "Microwave breast imaging using compressed sensing approach of iteratively corrected delay multiply and sum beamforming." *Diagnostics* 11, no. 3 (2021): 470. https://doi.org/10.3390/diagnostics11030470

[23] Schofield, R., L. King, U. Tayal, I. Castellano, J. Stirrup, F. Pontana, James Earls, and E. Nicol. "Image reconstruction: Part 1–understanding filtered back projection, noise and image acquisition." *Journal of cardiovascular computed tomography* 14, no. 3 (2020): 219-225. https://doi.org/10.1016/j.jcct.2019.04.008